

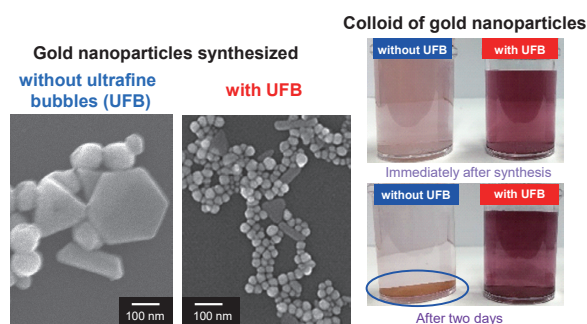
Characteristics of Ultrafine Bubbles (Bulk Nanobubbles) and Their Application to Particle-Related Technology[†]

Keiji Yasuda

Department of Chemical Systems Engineering, Nagoya University, Japan

Ultrafine bubbles (bulk nanobubbles), small bubbles with a diameter of less than 1 μm , have attracted academic and industrial attention because of their numerous advantages, including their chemical-free nature and extraordinarily long lifetime. The long lifetime is related to the much higher Brownian motion velocity compared to buoyancy. The reason why ultrafine bubbles can endure under stable conditions is still unclear, even though their inside is highly pressured. They have several characteristics, such as pH-dependent surface charge and reduced friction. They are also closely related to ultrasound. Ultrafine bubbles are generated and removed by selecting the ultrasonic frequency. Reaction and separation using ultrasonic cavitation and atomization, respectively, are enhanced by ultrafine bubbles. They can produce hollow nanoparticles, enhance adsorption on activated carbon, and clean solid surfaces. This review discusses the fundamental and ultrasonic characteristics of ultrafine bubbles and their application in particle-related technology, encompassing fine particle synthesis, adsorption, desorption, extraction, cleaning, and prevention of fouling.

Keywords: ultrafine bubbles, bulk nanobubbles, ultrasound, sonochemistry, fine particle synthesis, cleaning



1. Introduction

Submicron-sized bubbles have attracted academic and industrial interest lately. Although these floating bubbles in a liquid have previously been referred to as “nanobubbles” or “bulk nanobubbles,” the International Organization for Standards (ISO) decided in 2017 that these bubbles less than 1 μm in diameter be termed “ultrafine bubbles” (ISO 20480-1, 2017). Therefore, this review will refer to nanobubbles and bulk nanobubbles as ultrafine bubbles. Furthermore, bubbles between 1 and 100 μm in diameter are termed microbubbles, and ultrafine bubbles and microbubbles are collectively termed fine bubbles.

Ultrafine bubbles and microbubbles are liquid-floating bubbles with the entire bubble interface surrounded by liquid. Microbubbles in water appear cloudy, like milk, while ultrafine bubbles are transparent because they do not scatter visible light. Surface nanobubbles, on the other hand, are small bubbles with one side of the bubble interface in contact with liquid and the other side attached to the solid wall (Lohse and Zhang, 2015). The surface nanobubbles are spherical caps with heights ranging from a few nanometers to tens of nanometers and widths of about 1 μm . They do not move from a solid wall.

The rising velocity U of fine bubbles (microbubbles and ultrafine bubbles) in liquid due to buoyancy depends on the diameter of fine bubbles d and the physical properties of liquid and is expressed by the following Stokes equation (Stokes, 1851),

$$U = \frac{d^2(\rho_L - \rho_G)g}{18\mu} \quad (1)$$

where ρ_L and ρ_G are liquid and gas densities, respectively, μ is the liquid viscosity, and g is the gravitational acceleration. The Stokes equation is known to accurately represent the setting motion of a solid sphere in a liquid when the Reynolds number is less than 2. Experimental results of the rising velocity of microbubbles agree with those calculated using Eqn. (1) (Takahashi, 2005; Lee and Kim, 2005). However, ultrafine bubbles are subject to intense Brownian motion, like solid colloidal particles, due to collisions caused by the thermal motion of liquid molecules. The following Stokes–Einstein equation expresses the displacement of spherical particles using Brownian motion at low Reynolds numbers (Einstein, 1905).

$$\langle \Delta x^2 + \Delta y^2 + \Delta z^2 \rangle = \frac{2kTt}{\pi\mu d} \quad (2)$$

where $\langle \Delta x^2 + \Delta y^2 + \Delta z^2 \rangle$ is the mean square displacement of the fine particles, k is the Boltzmann constant, T is the temperature, and t is the observation time. Fig. 1 shows the comparison between the rising velocity using Eqn. (1) and the average velocity of Brownian motion per 1 s and 100 s

[†] Received 17 October 2022; Accepted 19 December 2022
 J-STAGE Advance published online 25 March 2023
 Add: Furo-cho, Chikusa-ku, Nagoya 464-8603, Japan
 E-mail: yasuda.keiji@material.nagoya-u.ac.jp
 TEL: +81-52-789-3623

by Eqn. (2) in the range of bubbles diameters from 10 nm to 10 μm . When the temperature is 298.15 K, the liquid and gas are considered to be water and air, respectively, and the bubbles are expected to be perfectly spherical. In the case of ultrafine bubbles less than 100 nm, the average velocity of Brownian motion is much greater than the rising velocity. This means that the ultrafine bubbles are dominated by random motion in all directions compared to the rising motion. Due to this interesting behavior, the removal of ultrafine bubbles from the liquid surface is nearly negligible. If there is no collision between the bubbles or dissolution into the liquid, ultrafine bubbles remain for a long time.

Thus, ultrafine bubbles have various interesting properties, such as a very long lifetime in liquid, a charged

surface, and controllable bubble concentration using ultrasound. Therefore, they have been applied in many fields, including water treatment, medicine, and the food industry (English, 2022). This review explains the fundamental and ultrasonic characteristics of ultrafine bubbles and describes their applications to particle-related technologies.

2. Fundamental characteristics

2.1 Size, concentration, and zeta potential

Like colloidal particles in solution, the surface of ultrafine bubbles is charged. The size and concentration of ultrafine bubbles in a liquid are closely related to the zeta potentials of ultrafine bubbles. They are mainly affected by the pH of solution, concentration, and several types of inorganic ions and surfactants in water.

Nirmalkar et al. (2018b) prepared air-filled ultrafine bubbles from pure water at pH = 6.5 using hydrodynamic cavitation methods and then changed the pH of ultrafine bubbles water by HCl and NaOH. The size distribution and zeta potential of ultrafine bubbles were measured using nanoparticle tracking analysis (Patois et al., 2012) and electrophoresis, respectively. Fig. 2 shows the effects of pH on (a) size distribution, (b) number density (concentration), (c) mean diameter, and (d) zeta potential of ultrafine bubbles. When pH was higher than 4, the bubble size distribution did not significantly change. However, at pH below 4, the peak of the bubble size distribution decreased sharply. This is reflected in the sharp drop in the bubble

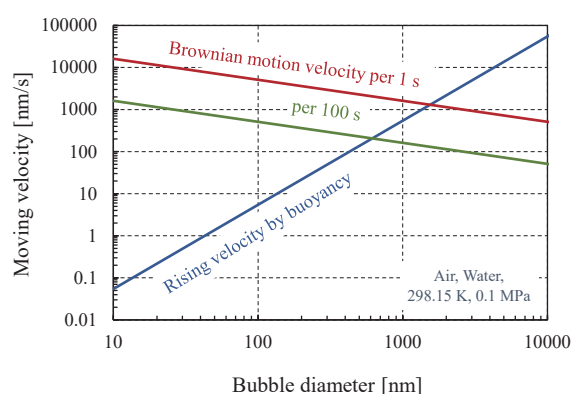


Fig. 1 Velocity comparison between Brownian motion and buoyancy.

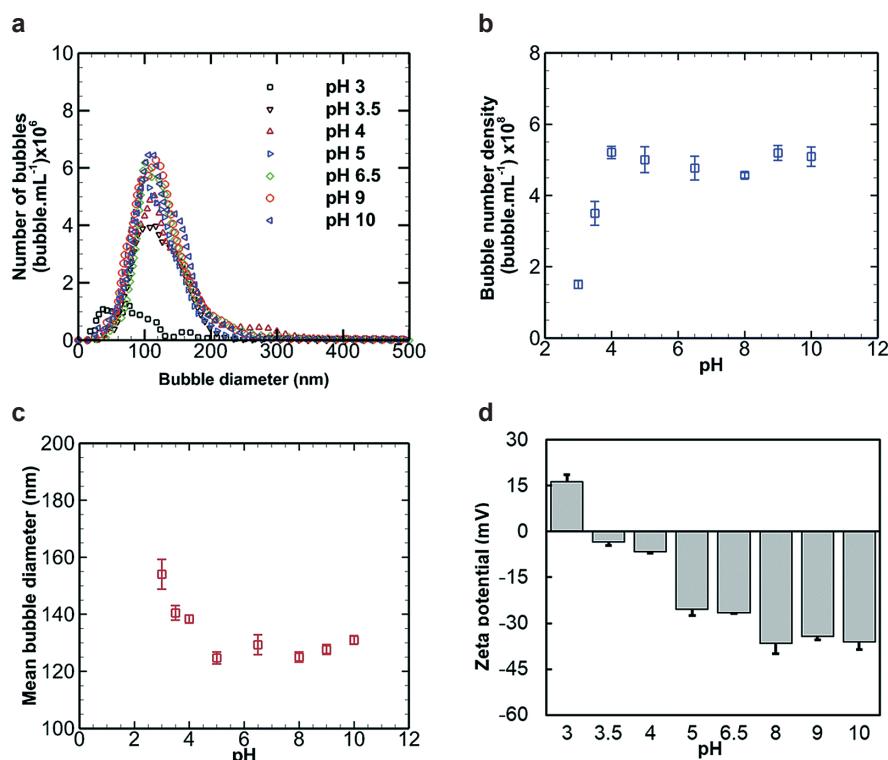


Fig. 2 Effects of pH on (a) size distribution, (b) concentration, (c) mean diameter, and (d) zeta potential of ultrafine bubbles. Reproduced with permission from Ref. (Nirmalkar et al., 2018b). Copyright: (2018) The Royal Society of Chemistry.

number concentration (density) as the pH decreased from 4 to 3. The mean bubble diameter increased significantly as the pH decreased below 4. The negative zeta potential of bubbles approached 0 with decreasing pH and became positive below the isoelectric point between pH 3 and 3.5. This is because the electrostatic repulsive force between ultrafine bubbles becomes weaker, bubbles agglomerate, and the bubble diameter increases, as the zeta potential is close to the isoelectric point. At the same time, excessively large bubbles rise and collapse at the gas–liquid interface, and the bubble concentration decreases. Other researchers have reported similar results with isoelectric points between pH 3 and 5 (Calgaroto et al., 2014; Azevedo et al., 2016; Bui et al., 2019; Ma et al., 2022).

Effects of NaCl concentration on properties of ultrafine bubbles have been widely reported (Millare and Basilia, 2018; Nirmalkar et al., 2018a, 2018b; Meegoda et al., 2018, 2019; Ke et al., 2019). Most of the data indicated that as the NaCl concentration increased, the bubble concentration decreased, the mean diameter increased, and the zeta potential approached zero. This is because sodium ions are adsorbed at the surface of the ultrafine bubble, and the zeta potential is close to zero. In the case of AlCl_3 , a trivalent cation, the zeta potential first approached zero and then changed to positive with increasing AlCl_3 concentration (Nirmalkar et al., 2018b). Hewage et al. (2021a) investigated the mean diameter and zeta potential of ultrafine bubbles in aqueous solutions for several inorganic salts.

The addition of cetyltrimethylammonium bromide, a cationic surfactant, changed the zeta potential from negative to positive, as in the case of AlCl_3 (Nirmalkar et al., 2018b; Agarwal et al., 2022). On the other hand, adding sodium dodecyl sulfate, an anionic surfactant, further decreased the zeta potential (Phan et al., 2021b). The addition of nonionic surfactants had a little significant effect on the zeta potential (Nirmalkar et al., 2018b). These experimental results of surfactant addition were explained using the adsorption of surfactants on ultrafine bubbles due to hydrophobic attraction. Effects of gas types inside ultrafine bubbles have been reported (Meegoda et al., 2018; Zhou et al.,

2021). For air, nitrogen, oxygen, and ozone gases, it was explained that the bubble size increased with increasing gas solubility in water and the zeta potential depended on the ability of the gas to produce OH^- ions at the water–gas interface (Meegoda et al., 2018).

The ultrafine bubbles in water were concentrated without loss and size change when water was evaporated from ultrafine bubble water under reduced pressure using a rotary evaporator (Tanaka et al., 2020). Additionally, ultrafine bubbles in water were diluted by gently adding pure water without loss and size change of ultrafine bubbles. A facile membrane-based physical sieving method was developed to make the ultrafine bubbles in targeting size (Zhang R. et al., 2022b). They used several membranes consisting of six different materials with pore diameters of 0.22 and 0.45 μm . The size distribution of the ultrafine bubbles could be intentionally adjusted by selecting the membrane and filtration rate. The ability to control the concentration and size of ultrafine bubble will be important for future application development.

2.2 Stability

The unique property of ultrafine bubbles is their unusually long lifetime. Ultrafine bubbles, once formed, are highly persistent (Zimmerman et al., 2011) and stable for days (Ohgaki et al., 2010; Ushikubo et al., 2010; Liu et al., 2013) and even months (Duval et al., 2012; Nirmalkar et al., 2018a; Kanematsu et al., 2020; Soyuluoglu et al., 2021; Tanaka et al., 2021b).

Tanaka et al. (2021b) generated air-filled ultrafine bubbles from ultrapure water using the pressurized dissolution method and stored the ultrafine bubble water at 298 K for 74 days. The results showed little difference in the stability of ultrafine bubbles between 30 mL glass vials, 1 L glass bottles, and 20 L high-density polyethylene containers. Fig. 3 shows the effect of storage temperature on the stability of ultrafine bubbles in 30 mL glass vials. Although number concentration decreased with time, ultrafine bubbles still existed on day 74. This is because the translational velocity due to Brownian motion is considerably

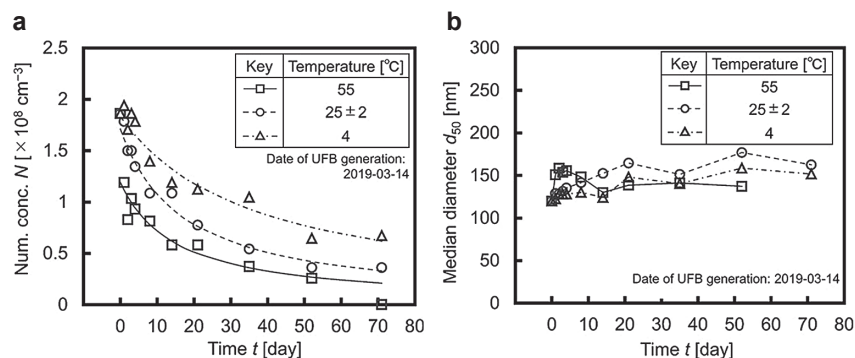


Fig. 3 Effect of storage temperature on the stability of ultrafine bubbles in 30 mL glass vials: **a**) number concentration and **b**) median diameter of ultrafine bubbles. Reprinted with permission from Ref. (Tanaka et al., 2021b). Copyright: (2021) John Wiley and Sons.

higher than the rising velocity due to buoyancy, as shown in Fig. 1. The stability became higher as the temperature decreased, and median diameter slightly increased with time. They explained that the Brownian motion of ultrafine bubbles became more active at higher temperatures and ultrafine bubbles tended to aggregate more easily. They expressed the stability of the ultrafine bubbles in terms of a second-order flocculation rate equation. Kanematsu et al. (2020) investigated the stability of ultrafine bubbles for 9 months at 298 K and reported that ultrafine bubbles were stable and zeta potential did not change significantly for 9 months.

Effects of additives on the long-term stability of oxygen ultrafine bubbles were investigated for 60 days (Soyluoglu et al., 2021). The bubble stability decreased with decreasing pH in the range of 3 to 9. The addition of Na^+ and Ca^{2+} ions reduced the stability. This is because the zeta potential of the ultrafine bubbles became close to 0, and the ultrafine bubbles tended to aggregate. Furthermore, the stability became low when the concentration of organic substances was high, but the effect of chlorine was small.

The boundary layer structure of ultrafine bubbles has been studied to elucidate the reason for their stability. Ohgaki et al. (2010) used attenuated total reflectance infrared spectroscopy to analyze and reported that the surfaces of the ultrafine bubbles contain hard hydrogen bonds that may reduce the diffusivity of gases through the interfacial film. Weijts et al. (2012) used molecular dynamics and concluded that ultrafine bubbles within a cluster of bubbles protect each other from diffusion by a shielding effect. Zhang X. et al. (2016) performed quantum computations and Raman spectrometric measurements. They proposed that an ultrafine bubble is more dynamically stable because the bubble is surrounded by a layer of supersolid skin. Hirai et al. (2019) studied the structure of ultrafine bubbles using small- and wide-angle X-ray scattering and explained that an ultrafine bubble is surrounded by a diffusive boundary, and the electron density differs between the diffusive boundary and the bulk solution. Zhang R. et al. (2022a) quantified the boundary layer thickness of the ultrafine bubbles using solvent relaxation of nuclear magnetic resonance. For effective gas diameters of 243.5, 358.5, and 412.8 nm, the determined boundary layer thicknesses were 41.5, 44.8, and 35.9 nm, and the ratios of the boundary layer thickness to the effective gas diameter were 0.17, 0.125, and 0.087, respectively.

The bubble was surrounded by water, which has high intermolecular forces, and the inner bubble was pressurized because it is a gas with a sparse density compared to the liquid. The pressure difference Δp is expressed using the Young–Laplace equation as follows (Attard, 2014),

$$\Delta p = p_{\text{in}} - p_{\text{out}} = \frac{2\sigma}{r} \quad (3)$$

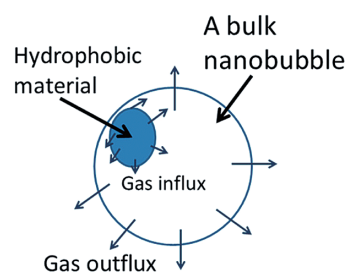


Fig. 4 Dynamic equilibrium model. Reprinted with permission from Ref. (Yasui et al., 2016). Copyright: (2016) American Chemical Society.

where p_{in} and p_{out} are the inner and outer pressure of the bubble, respectively and σ is the interfacial surface tension, and r is the bubble radius. Assuming that the interfacial tension at the macroscale and nanoscale is the same, the internal pressure of a bubble increases with decreasing bubble radius and becomes significantly high in the case of ultrafine bubbles. The inner pressure of bubbles becomes 2.98 MPa, when the bubble radius is 50 nm, the interfacial tension of water is 72 mN/m, and the outer pressure of the bubble is 0.1 MPa. The inner pressure of surface nanobubbles obtained using electrochemical measurement (German et al., 2016) and that of ultrafine bubbles estimated from the measurement of gas content in water (Kim E. et al., 2020) were consistent with the theoretical pressure values in Eqn. (3).

However, ultrafine bubbles are expected to dissolve immediately into the surrounding liquid because the pressure of the gas dissolved in a liquid is usually in the order of 0.1 MPa. The time for the complete dissolution of a bubble with 100 nm in radius is only about 80 μs according to the Epstein–Plesset theory (Epstein and Plesset, 1950; Yasui, 2015, 2018). Therefore, the lifetime of ultrafine bubbles should theoretically be very short, but in practice, as previously mentioned, it is very long.

Several stabilization models of ultrafine bubbles have been proposed to explain this discrepancy. Yasui et al. (2018) reviewed these models and supported the dynamic equilibrium model (Yasui et al., 2015, 2016; Brenner and Lohse, 2008; Petsev et al., 2013) because images of the transmission electron microscope showed stable ultrafine bubbles partly covered with hydrophobic materials in aqueous solutions (Sugano et al., 2017). Fig. 4 illustrates the dynamic equilibrium model. This model shows that a hydrophobic substance adheres to the bubble surface, and the gas concentrated on the surface of the hydrophobic substance flows into the bubble and is balanced by the amount of gas flowing out of the bubble in the rest of the bubble. However, the high stability of ultrafine bubbles must be investigated further, both experimentally and theoretically, to obtain a consistent conclusion in the future.

2.3 Other characteristics

Other characteristics of ultrafine bubbles include a

reduction in solution viscosity (Phan et al., 2021a), a reduction in friction (Ushida et al., 2012a; Nakagawa et al., 2022), and the generation of radicals.

Viscosities of apple juice concentrate and canola oil were examined after they were injected with CO₂ ultrafine bubbles with sizes ranging from 50 to 850 nm (Phan et al., 2021a). A significant viscosity reduction was observed by up to 18 % and 10 % in apple juice concentrate and canola oil, respectively. The pressure drop across a micro-orifice was measured using water and glycerol aqueous solutions containing ultrafine bubbles (Ushida et al., 2012a). The friction reduction was observed for orifice diameters of 50 μm or less. This was because the ultrafine bubbles adhered to the wall surface, forming a gas phase that resulted in wall slip. The reduction of friction factor in an acrylic pipe with glass beads increased with an increasing number of ultrafine bubbles (Nakagawa et al., 2022). They explained that ultrafine bubbles filled more undulated space and made the rough surface smoother.

Free radicals, including hydroxyl radicals, were detected in ultrafine bubble water (Minamikawa et al., 2015; Liu et al., 2016a, b; Atkinson et al., 2019). Free radicals are believed to be formed through the collapse of ultrafine bubbles (Takahashi et al., 2021). Soyluoglu et al. (2021) reported that hydroxyl radicals in oxygen ultrafine bubble solutions were detected at pH 3 but were little detected at pH 6.5. Yasui et al. (2018) discussed the generation possibility of hydroxyl radicals from air ultrafine bubbles using numerical simulations. They suggested that hydroxyl radicals formed due to hydrodynamic cavitation in producing ultrafine bubbles.

3. Ultrasonic characteristics

3.1 Ultrasonic cavitation

When water is irradiated with ultrasound, fine bubbles are generated from bubble nuclei, grow to a resonance size through rectified diffusion (Ashokkumar et al., 2007; Crum, 1980) and collapse by semi-adiabatic compression (Leighton, 1994; Yasui, 2015). This phenomenon is called ultrasonic cavitation. By collapsing fine bubbles, the field inside the fine bubbles becomes high temperature and pressure, generating various radical species, which produces chemical effects (Suslick, 1990). Simultaneously, the collapse of fine bubbles generates jet flow and shock wave (Lauterborn and Ohl, 1997), producing mechanical effects.

Examples of the chemical effects include the decomposition of harmful substances (Pétrier et al., 1994; Yasuda, 2021) and the synthesis of metal nanoparticles (Gedanken, 2004; Sakai et al., 2009). However, examples of the mechanical effects include ultrasonic cleaning (Muthukumaran et al., 2005; Mason, 2016), ultrasonic emulsification (Beal and Skauen, 1955; Yasuda et al., 2012), and ultrasonic atomization (Wood and Loomis, 1927; Sato et al., 2001). Mechanical effects have been used

to develop commercial products such as cleaners, homogenizers, and atomizers. Usually, plate-type transducers are used for ultrasonic cleaners and atomizers, while horn-type transducers are used for ultrasonic homogenizers. Thus, ultrasound is closely related to ultrafine bubbles, and many studies using ultrasound have been reported.

3.2 Generation and removal of ultrafine bubbles

Ultrafine bubbles were generated using ultrasonic cleaner at 42 kHz (Kim J.-Y. et al., 2000) and ultrasonic homogenizer at 20 kHz (Cho et al., 2005; Nirmalkar et al., 2018a, 2019; Li et al., 2021; Lee and Kim, 2022b; Ma et al., 2022). Their generation rate increased with increased dissolved air content in pure water (Nirmalkar et al., 2018a). Studies have used several plate-type transducers to change ultrasonic frequencies ranging from 20 kHz to 1 MHz and to generate ultrafine bubbles in ultrapure water (Yasuda et al., 2019). **Figs. 5(a) and (b)** show the effect of ultrasonic frequency on the generation rate and mode diameter of ultrafine bubbles. The generation rate increased with decreasing frequency because cavitation collapse became stronger at lower frequencies. However, the mode diameters of ultrafine bubbles were 90–100 nm regardless of the frequency. The diameter, zeta potential, and stability of ultrafine bubbles generated using ultrasound are almost identical to those generated by hydrodynamic cavitation (Jadhav and Brigou, 2020), which is a commonly used method. The ultrasound method has the advantage of small sample volumes and the ability to generate ultrafine bubbles in variety of liquids, including organic solvents (Nirmalkar et al., 2019), inorganic solutions (Ma et al., 2022), and surfactant solutions (Lee and Kim, 2022a).

Removing ultrafine bubbles from liquid media is important to distinguish them from nanoparticles. The freeze-thawing method is often used to remove ultrafine bubbles in pure water. However, this method little removes ultrafine bubbles in the surfactant solution (Nirmalkar et al., 2018a), and it is time-consuming. Ultrasound has been irradiated at various frequencies to highly concentrated ultrafine bubble water produced using the pressurized dissolution method (Yasuda et al., 2019). **Fig. 5(c)** shows the effect of ultrasonic frequency on the removal rate of ultrafine bubbles. The removal rate increased with increasing frequency because the secondary Bjerknes force, an attraction between bubbles, increased. We modeled the formation and removal of ultrafine bubbles using ultrasound and discovered that ultrafine bubbles reach a frequency-dependent equilibrium concentration (**Fig. 5(d)**), regardless of the ultrasound intensity. Tanaka et al. (2021a) confirmed the ultrasonic removal of ultrafine bubbles using indirect irradiation. The ultrasonic frequency was 1.6 MHz, and ultrafine bubbles dispersions were prepared using two different bubble generator methods: pressurized dissolution and swirling liquid flow. Results showed that the indirect ultrasonic irradiation

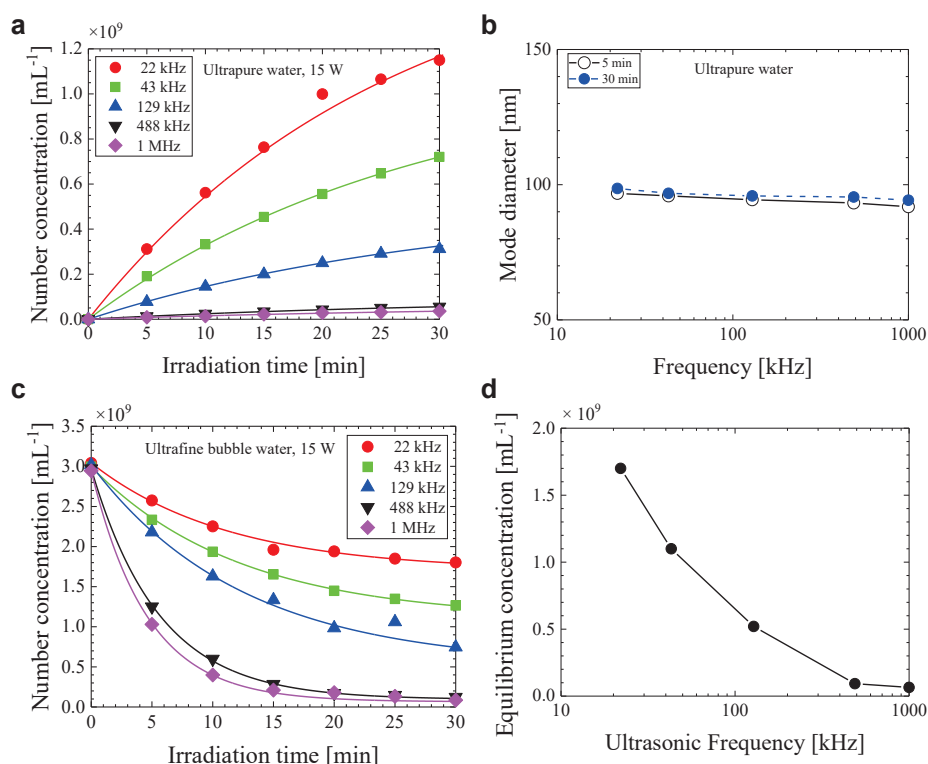


Fig. 5 Effect of ultrasonic frequency on (a) generation rate, (b) mode diameter, (c) removal rate, and (d) equilibrium concentrations of ultrafine bubbles.

for 30 min reduced the number concentration of ultrafine bubbles by 90 % regardless of the generation method. Feasibility studies were also conducted for ultrafine bubbles in an aqueous surfactant solution or solid particle dispersion. The ultrasonic method selectively destabilized ultrafine bubbles in the solutions. Ultrafine bubble removal using ultrasound has been adopted as an international standard by the International Organization for Standardization (ISO 24261-2, 2021) because of its simplicity and quickness of operation.

3.3 Sonochemical characteristics

Sonochemistry is a field in chemistry, physics, and biology related to ultrasonic cavitation. Some reports have shown that ultrafine bubbles promote ultrasonic cavitation (Tuziuti et al., 2020, 2021; Tsuchida et al., 2022). Sonoluminescence, which is light emission from a liquid due to ultrasonic cavitation (Brenner et al., 2002; Ashokkumar, 2011), was enhanced by ultrafine bubbles when ultrasound was applied at 54 kHz with high intensity (Tuziuti et al., 2020). This phenomenon was observed for various bubble concentrations (Tuziuti et al., 2021). They considered that ultrafine bubbles had the potential to provide nucleation sites for ultrasonic cavitation. The sonochemical degradation of acid orange was accelerated when the microbubble solution was irradiated with ultrasound at 45 kHz (Tsuchida et al., 2022). They concluded that ultrafine bubbles played an important role in improving sonochemical reactions.

An in-situ sediment remediation method using a combination of ultrasound and ozone ultrafine bubbles was investigated to remediate both organic (p-terphenyl) and inorganic (chromium) materials in contaminated sediments of the lower Passaic River in United States (Batagoda et al., 2019; Hewage et al., 2020, 2021b). The ozone ultrafine bubbles increased the solubility of ozone in water and reduced wastage. Also, the high-ozone concentration in water also increases chromium oxidation (Batagoda et al., 2019). This proposed treatment method showed sufficient remediation success with removing these combined contaminants, on average, 60 % and 71 % for p-terphenyl and chromium, respectively. The chromium removal was directly influenced by the chemical oxidation and sonication for chromium desorption from sediments. However, p-terphenyl degradation was more likely influenced by the combined effects of chemical oxidation and ultrasound-assisted pyrolysis (Hewage et al., 2021b). Dark green Rit dye was effectively decolorized by combining ultrafine bubbles and ultrasonic irradiation (Bui and Han, 2020). The color removal mechanisms were due to the electrostatic attraction between the ultrafine bubble and dye and the oxidation of the dye using reactive species such as hydroxy radicals generated through ultrasonic cavitation.

Ultrasonic atomization generates a mist, such as fine droplets at room temperature (Wood and Loomis, 1927; Yasuda et al., 2011). When an aqueous ethanol solution is atomized using ultrasound, the ethanol is enriched in the

mist (Sato et al., 2001; Yasuda et al., 2003; Matsuura et al., 2007). Ethanol enrichment is attributed to the hydrophobic interaction of ethanol molecules in water (Yasuda et al., 2014). Separation using ultrasonic atomization has also been reported on ketones (Yasuda et al., 2004), amino acids (Suzuki et al., 2006), surfactants (Jimmy et al., 2008), fine particles (Nii and Oka, 2014), and ion liquid (Mai et al., 2019). The advantages of ultrasonic atomization separation include simple operation, maintenance-free, and suitability for heat sensitive materials. Ultrafine bubbles water was used as a solvent to improve the enrichment performance using ultrasonic atomization (Yasuda et al., 2020b; 2022). The ethanol concentration in the collected mist with ultrafine bubbles was higher than that without ultrafine bubbles (Yasuda et al., 2020b). When the ethanol concentration in the solution was low and the carrier gas velocity was slow, the enrichment effect of ultrafine bubbles was particularly remarkable. Next, the enrichment characteristics of amino acids were investigated using ultrasonic atomization (Yasuda et al., 2022). Fig. 6 shows the effect of the concentration of amino acids in solution on the enrichment factor with and without ultrafine bubbles for L-phenylalanine and L-tyrosine. Here, the ratio of the solute concentration in the mist to that in the solution is defined as the enrichment factor. The enrichment factor increased with decreasing solution concentration and was enhanced by adding ultrafine bubbles. The authors explained the reason for this

enhancement as follows. Amino acid bonds to the surface of ultrafine bubbles in a solution because of their hydrophobic affinity. Under ultrasonic fields, ultrafine bubbles containing amino acids aggregate or coalesce by secondary Bjerknes force (Leighton, 1994), rise in the solution by buoyancy force and burst at the solution surface. The concentration of amino acids increases at the solution surface, and many amino acids are contained in the droplets.

Freezing of foods is a complicated and time-consuming process that requires the aggregation of molecules from a liquid to a solid crystal network (Kiani and Sun, 2011). The influences of CO₂ ultrafine bubbles and ultrasound on the crystallization behavior of water during freezing of model sugar solutions were examined (Adhikari et al., 2019). The combination treatment facilitated in reducing the supercooling degree, resulting in faster nucleation during the freezing process. This method may improve the characteristics of frozen products such as ice cream and frozen desserts.

4. Application to particle-related technologies

4.1 Fine particle synthesis

Synthesis of fine particles using ultrafine bubbles has been reported in several papers. Authors (Yasuda et al., 2020a) used HAuCl₄ aqueous solutions and synthesized gold nanoparticles by ultrasonic irradiation at 500 kHz with the aid of ultrafine bubbles without any capping and reducing agents. Figs. 7(a) and (b) show the electron micrographs and size distribution of gold nanoparticles synthesized with and without ultrafine bubbles. The particle sizes prepared with ultrafine bubbles were much smaller than those of the gold nanoparticles prepared without ultrafine bubbles. The mean diameter of the spherical gold nanoparticles synthesized with ultrafine bubbles decreased with increasing concentration of ultrafine bubbles. This is because ultrafine bubbles accelerate the sonochemical reduction of gold ions and suppress the aggregation between gold nanoparticles. Moreover, the gold nanoparticles were stable in a solution containing ultrafine bubbles (Fig. 7(c)) because gold nanoparticles were electrostatically adsorbed on ultrafine bubbles (Fig. 7(d)), which have a very long lifetime in water.

Nanocomposites of CaCO₃ and pulp fiber were prepared by injecting ultrafine bubbles of CO₂ into an aqueous Ca(OH)₂ solution containing pulp fibers (Fuchise-Fukuoka et al., 2020). The precipitated CaCO₃ nanoparticles formed on the pulp fiber surfaces were more stably attached to the pulp fiber surfaces against shear force. Compared with mixing method, the specific surface area and surface smoothness of nanosized CaCO₃-containing handsheets increased. Water containing ultrafine bubbles of hydrogen at high concentrations was used as the blending solvent for preparing cement mortar (Kim W.-K. et al., 2021). The cement mortar had greater flexural and compressive strengths

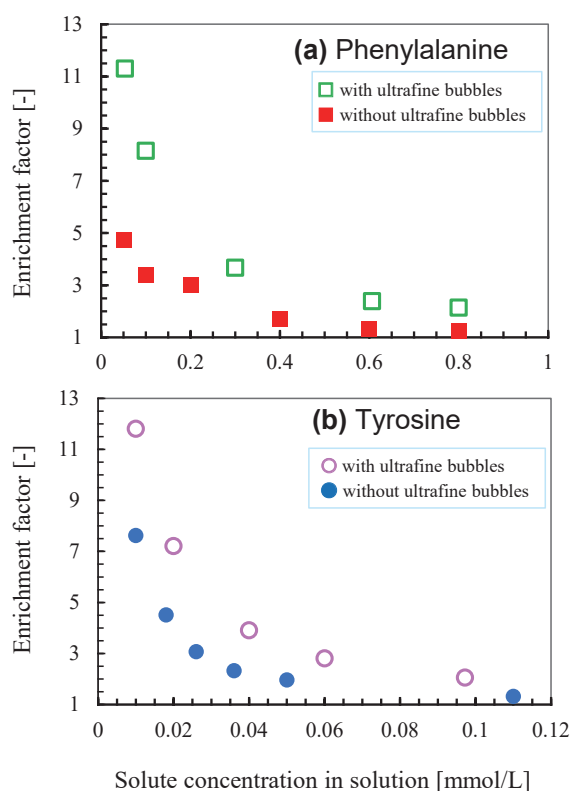


Fig. 6 Effect of solute concentration in solution on enrichment factor with and without ultrafine bubbles for (a) phenylalanine and (b) tyrosine.

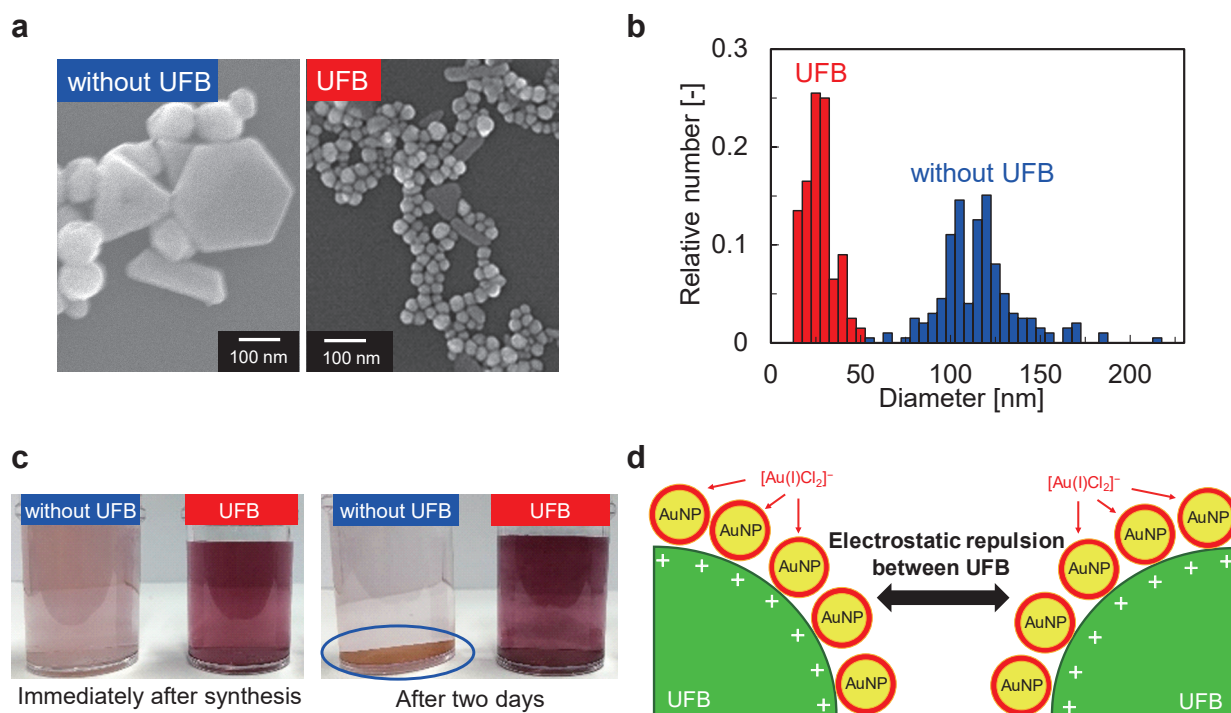


Fig. 7 Effect of ultrafine bubbles (UFB) on sonochemical synthesis and colloidal stability of gold nanoparticles: (a) Electron micrograph and (b) the size distribution of particles; (c) Photograph of colloids immediately and 2 days after synthesis; (d) Stabilization mechanism by ultrafine bubbles.

than plain water-based mortars. This was because ultrafine bubbles enhanced the collision between the solvent and cement particles, accelerating the hydration and pozzolanic reactions.

Jadhav and Brigou (2020) formed the hollow zinc phosphate nanoparticles using ultrafine bubbles as shown in Fig. 8. First, zinc nitrate was added to the ultrafine bubble water to adsorb Zn^{2+} ions on the negatively charged surface of ultrafine bubbles. Next, by adding diammonium phosphate, the ultrafine bubbles served as nucleation sites for the subsequent reaction of Zn^{2+} with PO_4^{3-} ions. Finally, the pH of the solution was adjusted to 8.5 to precipitate zinc phosphate on the ultrafine bubble surfaces, forming hollow particles. The advantages of using ultrafine bubbles for fine particle synthesis are safety, low environmental loads, and no impurities in fine particles. Ultrafine bubbles, in particular, are optimal for creating fine hollow fine particles since there is no need to remove the core templates, which are generally employed with solid or liquid particles.

4.2 Adsorption, desorption, and extraction

Studies have been reported on the use of ultrafine bubbles to promote adsorption onto particles, as well as desorption and extraction from particles. The effect of ultrafine bubbles on the adsorption of lead ions onto activated carbon was investigated with and without agitation (Kyzas et al., 2019; 2020). In the case of agitation, the effect of ultrafine bubbles on the adsorption capacity of lead ions was small. However, in the case without agitation, the

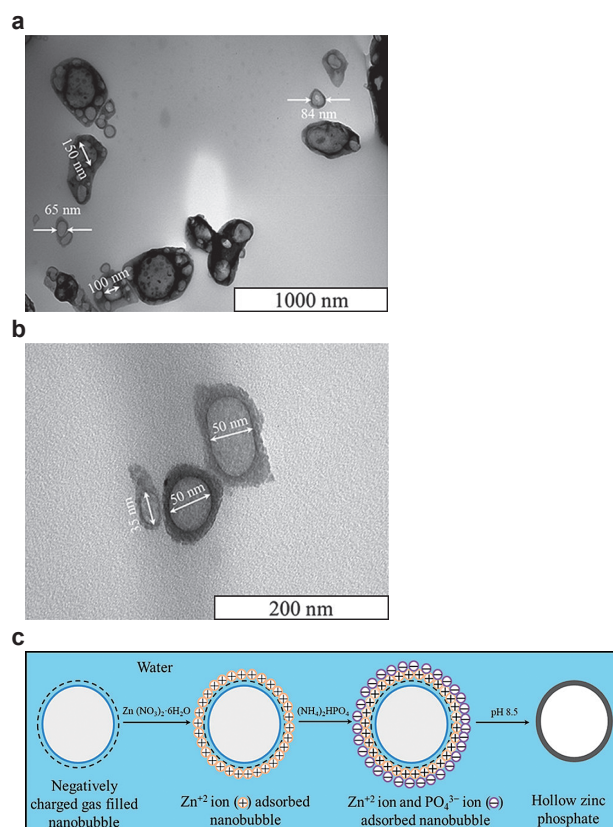


Fig. 8 Images of transmission electron microscopy of hollow zinc phosphate nanoparticles obtained by encapsulation of ultrafine bubbles shown on different scales: (a) 1000 nm; (b) 200 nm; (c) schematic representation of the formation of the hollow nanoparticles. Reprinted with permission from Ref. (Jadhav and Brigou, 2020). Copyright: (2020) American Chemical Society.

adsorption capacity in the presence of ultrafine bubbles became much higher than that in the absence of ultrafine bubbles. Moreover, ultrafine bubbles largely accelerated the adsorption rate with and without agitation. They explained that the ultrafine bubbles accepted positively charged lead ions onto their interface and assisted the diffusion and penetration phenomena of lead ions into the activated carbon pores. The influence of ultrafine bubbles on the adsorption of sodium oleate on calcite surface was examined (Wang et al., 2019). Ultrafine bubbles had a certain inhibitory effect on the adsorption of sodium oleate on the calcite surface, and it significantly promoted the flocculation between particles of sodium oleate.

Hydrogen ultrafine bubbles were applied to soils contaminated with copper to desorb copper (Kim and Han, 2020). Ultrafine bubbles improved the desorption of copper. Additionally, when the ultrafine bubbles were used as desorption enhancers in electrokinetic experiments, they had better remediation effects than distilled water.

Ettoumi et al. (2022) generated ultrafine bubbles in ion liquid using compression–decompression method and extracted polyphenols from Chinese Hickory. Compared to the extract using ion liquid without ultrafine bubbles, the extract of this method showed significantly higher antioxidant activity and polyphenol yields. Electron micrographs confirmed that nanojets due to ultrafine bubbles caused morphological destruction of the husk powder. Their group also extracted phytochemical compounds from *Camellia Oleifera* shells using water with CO₂ ultrafine bubbles (Javed et al., 2022). Compared with ethanol extraction, ultrafine bubble water led to a higher extraction yield of total phenolic and flavonoid content. Collagen was extracted from tilapia scales by bubbling ultrafine bubbles of three different gases (O₂, CO₂, and O₃) into an acetic acid solution (Kuwahara, 2021). Using CO₂ in the acetic acid solution was the most effective method to obtain collagen in a relatively high yield. The ultrafine bubble method is a simple, mild, cost-effective, and environmentally friendly method for adsorption onto particles, as well as desorption and extraction from particles.

4.3 Cleaning and prevention of fouling

The most typical application of ultrafine bubbles is cleaning. There are several reports on the use of ultrafine bubbles to remove contaminants from solid surfaces. Minute particles with a diameter of about 50 nm were successfully removed from the wafer surfaces by impinging a jet of ultrapure water containing ultrafine bubbles (Morimatsu et al., 2004). Removal of protein from the solid–liquid interface was investigated using a quartz crystal microbalance to evaluate the removal amount (Liu et al., 2008; Liu and Craig, 2009). Bovine serum albumin was completely removed from both hydrophobic and hydrophilic surfaces using ultrafine bubbles. The cleaning efficiency compared

to sodium dodecyl sulfate, a typical surfactant (Liu et al., 2008). Lysozyme was completely removed from hydrophobic surfaces by combing ultrafine bubbles and sodium dodecyl sulfate (Liu and Craig, 2009). Ushida et al. (2012b) investigated the washing rate of cloth in an alternating flow system. The ultrafine bubble water achieved a washing rate greater than that of ion-exchanged water. Moreover, the mixture with ultrafine bubbles and anionic surfactant exhibited a washing rate higher than that of an aqueous anionic surfactant solution without ultrafine bubbles. The ceramic membrane completely clogged by humic acid fouling was effectively cleaned using ultrafine bubbles (Ghadimkhani et al., 2016). Dyed cotton towels were washed without soap using oxygen-rich ultrafine bubbles and with soap using the conventional method (Anis et al., 2022). The lowest color strength and highest fastness were obtained after washing with ultrafine bubbles. Chemical oxygen demand measurements of washing baths revealed that ultrafine bubble washing was more environmentally friendly than conventional methods.

Terasaka (2021) investigated the cleaning process of salt adhering to wall surfaces when ultrafine bubble water was passed through a sample surface at a constant flow rate. The cleaning rate was determined using the dissolved salt concentration in water. Fig. 9(a) shows the progress of the cleaning rate when “hard deposits,” such as salts, were washed with running water, as opposed to paste-like “soft deposits,” such as biofilm and starch. The cleaning process consists of adhesion, dissolution, peeling, and dissolution. The starting time of the peeling step is promoted by ultrafine bubbles, and consequently, the cleaning is completed in a shorter time with ultrafine bubble water. Fig. 9(b) shows a hypothesis of the cleaning mechanism. It explains that the cleaning mechanism using ultrafine bubbles uses the high permeability of ultrafine bubbles accompanying water and the metastability of ultrafine bubbles that shift to a stable state when the specific potential is exceeded. In 2011, West Nippon Expressway Company Limited started cleaning toilets in expressway service stations and parking areas using ultrafine bubbles. Ultrafine bubbles have been successfully used to remove salts from bridge surfaces. The necessary time for removing salt from the surface has shortened to less than one-fourth using a water jet containing ultrafine bubbles (Yabe, 2021).

Ultrafine bubbles were found to prevent surface fouling of bovine serum albumin (Wu et al., 2008) and lysozyme (Zhu et al., 2016). Farid et al. (2022) demonstrated the benefits of introducing ultrafine bubbles into the feed for alleviating flux reduction and membrane pore wetting associated with mineral scaling in membrane distillation. Introducing ultrafine bubbles reduced membrane scaling propensity and offered excellent resistance to pore wetting associated with scaling. This is attributed to high surface shear forces due to flow turbulence and electrostatic

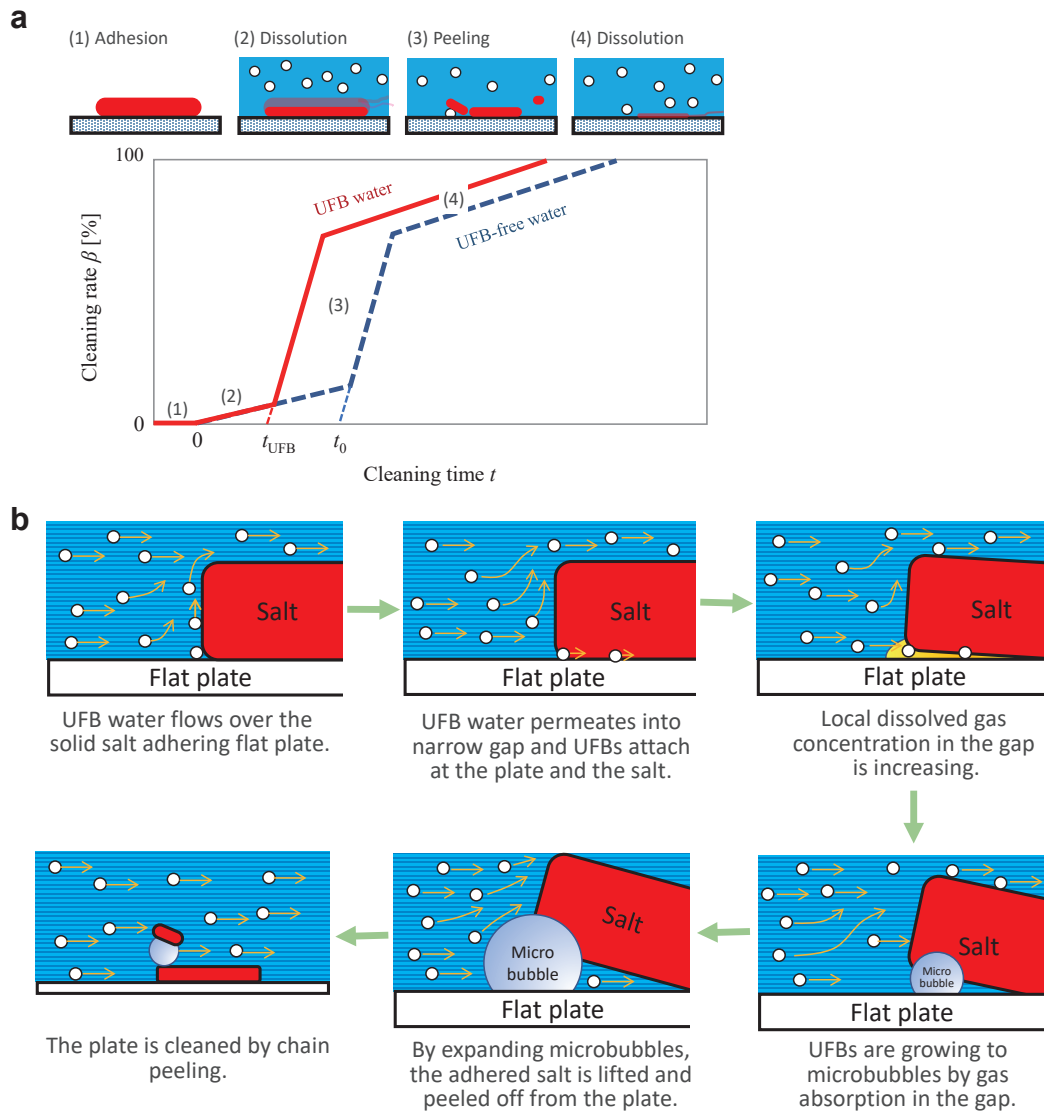


Fig. 9 (a) Cleaning process of salt adhering to wall surface with ultrafine bubble water and (b) hypothesis of removal mechanism of wall-attached salt by flowing ultrafine bubble water. Reprinted with permission from Ref. (Terasaka, 2021). Copyright: (2021) Jenny Stanford Publishing.

attractions between the negatively charged ultrafine bubbles and the counterions. The potential use of ultrafine bubbles as corrosion and scale inhibitors for geothermal power plants was discussed (Kioka and Nakagawa, 2021). The crystal growth rate of calcite, which causes scaling, was found to be more retarded as the concentration of ultrafine bubbles increased (Tagomori et al., 2022). Ultrafine bubbles inhibit the corrosion of low-carbon steels, with an inhibition efficiency of 20–50 % in the acidic geothermal fluid (Aikawa et al., 2021). They concluded that ultrafine bubbles could act as a nanoscopic coating material in mitigating corrosion, increasing the slip length on the solid interface and preventing exposing the interface to acidic geothermal fluids by (1) behaving as a bubble mattress covering most of the steel surface or (2) promoting nucleation and aggregation of an insignificant quantity of silica precipitation on the steel surface. Compared to commonly used chemical products, ultrafine bubbles have shown to

be a potent, chemically benign, environmentally friendly, and inexpensive corrosion and scale inhibitor of calcium carbonate.

5. Conclusions

This review discussed the fundamental and ultrasonic characteristics of ultrafine bubbles (bulk nanobubbles) and introduced their application to particle-related technology. The diameter of ultrafine bubbles is less than 1 μm , and the bubble surface is highly charged. The rising velocity due to buoyancy is much smaller than the Brownian motion velocity. The diameter and concentration are closely related to zeta potential. The diameter, concentration, and zeta potential of ultrafine bubbles depend on pH of solution, concentration, and several types of inorganic ions and surfactants in water. Additionally, the concentration can be increased using a rotary evaporator. They are stable in water for several months; however, there is no model

to fully explain the stabilization mechanism. They formed hydroxy radicals at strong acid conditions and reduced in friction in the orifice.

Ultrafine bubbles can be generated and removed using ultrasonic irradiation at low and high frequencies, respectively. Chemical and physical effects of ultrasonic cavitation, such as luminescence and degradation, were enhanced by ultrafine bubbles. It was considered that ultrafine bubbles became the nucleation of cavitation. Separation performance of ethanol and amino acids from aqueous solutions using ultrasonic atomization was improved by ultrafine bubbles.

Ultrafine bubbles have been applied to fine particle synthesis, adsorption, desorption, extraction, cleaning, and prevention of fouling. Fine gold nanoparticles, CaCO₃/pulp fiber nanocomposites, and hollow zinc phosphate nanoparticles were synthesized by ultrafine bubbles. Adsorption of lead ions to activated carbon and desorption of copper from soil were enhanced by ultrafine bubbles due to electrostatic interaction between ultrafine bubbles and metal ions. Bubbling CO₂ ultrafine bubbles effectively extracted collagen from tilapia scales. Ultrafine bubble water without surfactant efficiently cleaned the protein, dye, and salt on solid surfaces and prevented surface fouling. Thus, ultrafine bubbles have been shown to be powerful, environmentally friendly, safe, clean, simple, and inexpensive methods.

Currently, ultrafine bubbles have many theoretically unexplained characteristics, such as high stability and chargeability, and a great deal of academic research is still being conducted. Clarifying the various characteristics of ultrafine bubbles is expected to lead to academic development and further social and industrial diffusion of ultrafine bubbles through applied research, such as developing new applications in various fields and reducing production costs.

Acknowledgments

This work was partly supported by JSPS KAKENHI Grant Numbers JP16H04560 and JP19H02505.

References

- Adhikari B.M., Tung V.P., Truong T., Bansal N., Bhandari B., Water crystallisation of model sugar solutions with nanobubbles produced from dissolved carbon dioxide, *Food Biophysics*, 14 (2019) 403–414. DOI: 10.1007/s11483-019-09590-2
- Agarwal K., Trivedi M., Nirmalkar N., Bulk nanobubbles in aqueous salt solution, *Materials Today: Proceedings*, 57 (2022) 1789–1792. DOI: 10.1016/j.matpr.2021.12.477
- Aikawa A., Kioka A., Nakagawa M., Anzai S., Nanobubbles as corrosion inhibitor in acidic geothermal fluid, *Geothermics*, 89 (2021) 101962. DOI: 10.1016/j.geothermics.2020.101962
- Anis P., Toprak-Cavdur T., Çalıřkan N., Oxygen-enriched nanobubbles for a green reactive washing process, *AATCC Journal of Research*, 9 (2022) 152–160. DOI: 10.1177/24723444221084396
- Ashokkumar M., Lee J., Kentish S., Grieser F., Bubbles in an acoustic field: an overview, *Ultrasonics Sonochemistry*, 14 (2007) 470–475. DOI: 10.1016/j.ultsonch.2006.09.016
- Ashokkumar M., The characterization of acoustic cavitation bubbles—an overview, *Ultrasonics Sonochemistry*, 18 (2011) 864–872. DOI: 10.1016/j.ultsonch.2010.11.016
- Atkinson A.J., Apul O.G., Schneider O., Garcia-Segura S., Westerhoff P., Nanobubble technologies offer opportunities to improve water treatment, *Account of Chemical Research*, 52 (2019) 1196–1205. DOI: 10.1021/acs.accounts.8b00606
- Attard P., The stability of nanobubbles, *The European Physical Journal Special Topics*, 223 (2014) 893–914. DOI: 10.1140/epjst/e2013-01817-0
- Azevedo A., Etchepare R., Calgaroto S., Rubio J., Aqueous dispersions of nanobubbles: generation, properties and features, *Minerals Engineering*, 94 (2016) 29–37. DOI: 10.1016/j.mineng.2016.05.001
- Batagoda J.H., Hewage S.D.A., Meegoda J.N., Remediation of heavy-metal-contaminated sediments in USA using ultrasound and ozone nanobubbles, *Journal of Environmental Engineering and Science*, 14 (2019) 130–138. DOI: 10.1680/jenes.18.00012
- Beal H.M., Skauen D.M., A study of emulsification with ultrasonic waves II, *Journal of the American Pharmaceutical Association*, 44 (1955) 490–493. DOI: 10.1002/jps.3030440810
- Brenner M.P., Hilgenfeldt S., Lohse D., Single-bubble sonoluminescence, *Reviews of Modern Physics*, 74 (2002) 425–484. DOI: 10.1103/RevModPhys.74.425
- Brenner M.P., Lohse D., Dynamic equilibrium mechanism for surface nanobubble stabilization, *Physical Review Letters*, 101 (2008) 214505. DOI: 10.1103/PhysRevLett.101.214505
- Bui T.T., Nguyen D.C., Han M., Average size and zeta potential of nanobubbles in different reagent solutions, *Journal of Nanoparticles Research*, 21 (2019) 173. DOI: 10.1007/s11051-019-4618-y
- Bui T.T., Han M., Decolorization of dark green Rit dye using positively charged nanobubbles technologies, *Separation and Purification Technology*, 233 (2020) 116034. DOI: 10.1016/j.seppur.2019.116034
- Calgaroto S., Wilberg K.Q., Rubio J., On the nanobubbles interfacial properties and future applications in flotation, *Minerals Engineering*, 60 (2014) 33–40. DOI: 10.1016/j.mineng.2014.02.002
- Cho S.-H., Kim J.-Y., Chun J.-H., Kim J.-D., Ultrasonic formation of nanobubbles and their zeta-potentials in aqueous electrolyte and surfactant solutions, *Colloids and Surfaces A: Physicochemical and Engineering Aspects*, 269 (2005) 28–34. DOI: 10.1016/j.colsurfa.2005.06.063
- Crum L.A., Measurements of the growth of air bubbles by rectified diffusion, *The Journal of the Acoustical Society of America*, 68 (1980) 203–211. DOI: 10.1121/1.384624
- Duval E., Adichtchev S., Sirotkin S., Mermet A., Long-lived submicrometric bubbles in very diluted alkali halide water solutions, *Physical Chemistry Chemical Physics*, 14 (2012) 4125–4132. DOI: 10.1039/c2cp22858k
- Einstein A., Über die von der molekularkinetischen Theorie der Wärme geforderte Bewegung von in ruhenden Flüssigkeiten suspendierten Teilchen, *Annalen der Physik*, 322 (1905) 549–560. DOI: 10.1002/andp.19053220806
- English N.J., Environmental exploration of ultra-dense nanobubbles: rethinking sustainability, *Environments*, 9 (2022) 33. DOI: 10.3390/environments9030033
- Epstein P.S., Plesset M.S., On the stability of gas bubbles in liquid-gas solutions, *The Journal of Chemical Physics*, 18 (1950) 1505–1509. DOI: 10.1063/1.1747520
- Ettoumi F.-E., Zhang R., Belwal T., Javed M., Xu Y., Li L., Weide L., Luo Z., Generation and characterization of nanobubbles in ionic liquid for a green extraction of polyphenols from *Carya cathayensis* Sarg., *Food Chemistry*, 369 (2022) 130932. DOI: 10.1016/j.foodchem.2021.130932
- Farid M.U., Kharraz J.A., Lee C.-H., Fang J.K.-H., St-Hilaire S., An A.K., Nanobubble-assisted scaling inhibition in membrane distillation for the treatment of high-salinity brine, *Water Research*, 209 (2022) 117954. DOI: 10.1016/j.watres.2021.117954
- Fuchise-Fukuoka M., Oishi M., Goto S., Isogai A., Preparation of CaCO₃ nanoparticle/pulp fiber composites using ultrafine bubbles, *Nordic*

- Pulp & Paper Research Journal, 35 (2020) 279–287. DOI: 10.1515/nppj-2019-0078
- Gerdenken A., Using sonochemistry for the fabrication of nanomaterials, *Ultrasonics Sonochemistry*, 11 (2004) 47–55. DOI: 10.1016/j.ultrsonch.2004.01.037
- German S.R., Edwards M.A., Chen Q., White H.S., Laplace pressure of individual H₂ nanobubbles from pressure-addition electrochemistry, *Nano Letters*, 16 (2016) 6691–6694. DOI: 10.1021/acs.nanolett.6b03590
- Ghadimkhani A., Zhang W., Marhaba T., Ceramic membrane defouling (cleaning) by air nano bubbles, *Chemosphere*, 146 (2016) 379–384. DOI: 10.1016/j.chemosphere.2015.12.023
- Hewage S.A., Batagoda J.H., Meegoda J.N., In situ remediation of sediments contaminated with organic pollutants using ultrasound and ozone nanobubbles, *Environmental Engineering Science*, 37 (2020) 521–534. DOI: 10.1089/ees.2019.0497
- Hewage S.A., Kewalramani J., Meegoda J.N., Stability of nanobubbles in different salts solutions, *Colloids and Surfaces A*, 609 (2021a) 125669. DOI: 10.1016/j.colsurfa.2020.125669
- Hewage S.A., Batagoda J.H., Meegoda J.N., Remediation of contaminated sediments containing both organic and inorganic chemicals using ultrasound and ozone nanobubbles, *Environmental Pollution*, 274 (2021b) 116538. DOI: 10.1016/j.envpol.2021.116538
- Hirai M., Ajito S., Takahashi K., Iwasa T., Li X., Wen D., Kawai-Hirai R., Ohta N., Igarashi N., Shimizu N., Structure of ultrafine bubbles and their effects on protein and lipid membrane structures studied by small- and wide-angle X-ray scattering, *The Journal of Physical Chemistry B*, 123 (2019) 3421–3429. DOI: 10.1021/acs.jpcc.9b00837
- ISO 20480-1:2017, Fine bubble technology—General principles for usage and measurement of fine bubbles—Part 1: Terminology, (2017). <<https://www.iso.org/standard/68187.html>> accessed 20.12.2022.
- ISO 24261-2:2021, Fine bubble technology—Elimination method for sample characterization—Part 2: Fine bubble elimination techniques, (2021). <<https://www.iso.org/standard/80020.html>> accessed 20.12.2022.
- Jadhav A.J., Brigou M., Bulk nanobubbles or not nanobubbles: that is the question, *Langmuir*, 36 (2020) 1699–1708. DOI: 10.1021/acs.langmuir.9b03532
- Javed M., Belwal T., Ruyuan Z., Xu Y., Li L., Luo Z., Optimization and mechanism of phytochemicals extraction from *Camellia Oleifera* shells using novel biosurfactant nanobubbles solution coupled with ultrasonication, *Food and Bioprocess Technology*, 15 (2022) 1101–1114. DOI: 10.1007/s11947-022-02793-5
- Jimmy B., Kentish S., Grieser F., Ashokkumar M., Ultrasonic nebulization in aqueous solutions and the role of interfacial adsorption dynamics in surfactant enrichment, *Langmuir*, 24 (2008) 10133–10137. DOI: 10.1021/la801876s
- Kanematsu W., Tuziuti T., Yasui K., The influence of storage conditions and container materials on the long term stability of bulk nanobubbles—consideration from a perspective of interactions between bubbles and surroundings, *Chemical Engineering Science*, 219 (2020) 115594. DOI: 10.1016/j.ces.2020.115594
- Ke S., Xiao W., Quan N., Dong Y., Zhang L., Hu J., Formation and stability of bulk nanobubbles in different solutions, *Langmuir*, 35 (2019) 5250–5256. DOI: 10.1021/acs.langmuir.9b00144
- Kiani H., Sun D.-W., Water crystallization and its importance to freezing of foods: a review, *Trends in Food Science & Technology*, 22 (2011) 407–426. DOI: 10.1016/j.tifs.2011.04.011
- Kim D., Han J., Remediation of copper contaminated soils using water containing hydrogen nanobubbles, *Applied Sciences*, 10 (2020) 2185. DOI: 10.3390/app10062185
- Kim E., Choe J.K., Kim B.H., Kim J., Park J., Choi Y., Unraveling the mystery of ultrafine bubbles: establishment of thermodynamic equilibrium for sub-micron bubbles and its implications, *Journal of Colloid and Interface Science*, 570 (2020) 173–181. DOI: 10.1016/j.jcis.2020.02.101
- Kim J.-Y., Song M.-G., Kim J.-D., Zeta potential of nanobubbles generated by ultrasonication in aqueous alkyl polyglycoside solutions, *Journal of Colloid and Interface Science*, 223 (2000) 285–291. DOI: 10.1006/jcis.1999.6663
- Kim W.-K., Hong G., Kim Y.-H., Kim J.-M., Kim J., Han J.-G., Lee J.-Y., Mechanical strength and hydration characteristics of cement mixture with highly concentrated hydrogen nanobubble water, *Materials*, 14 (2021) 2735. DOI: 10.3390/ma14112735
- Kioka A., Nakagawa M., Theoretical and experimental perspectives in utilizing nanobubbles as inhibitors of corrosion and scale in geothermal power plant, *Renewable and Sustainable Energy Reviews*, 149 (2021) 111373. DOI: 10.1016/j.rser.2021.111373
- Kuwahara J., Extraction of type I collagen from tilapia scales using acetic acid and ultrafine bubbles, *Processes*, 9 (2021) 288. DOI: 10.3390/pr9020288
- Kyzas G.Z., Bomis G., Kosheleva R.I., Eftimiadou E.K., Favvas E.P., Kostoglou M., Mitropoulos A.C., Nanobubbles effect on heavy metal ions adsorption by activated carbon, *Chemical Engineering Journal*, 356 (2019) 91–97. DOI: 10.1016/j.cej.2018.09.019
- Kyzas G.Z., Favvas E.P., Kostoglou M., Mitropoulos A.C., Effect of agitation on batch adsorption process facilitated by using nanobubbles, *Colloids and Surfaces A*, 607 (2020) 125440. DOI: 10.1016/j.colsurfa.2020.125440
- Lauterborn W., Ohl C.-D., Cavitation bubble dynamics, *Ultrasonics Sonochemistry*, 4(1997)65–75. DOI: 10.1016/S1350-4177(97)00009-6
- Lee J.I., Kim J.-M., Role of anionic surfactant in the generation of bulk nanobubbles by ultrasonication, *Colloid and Interface Science Communications*, 46 (2022a) 100578. DOI: 10.1016/j.colcom.2021.100578
- Lee J.I., Kim J.-M., Influence of temperature on bulk nanobubble generation by ultrasonication, *Colloid and Interface Science Communications*, 49 (2022b) 100639. DOI: 10.1016/j.colcom.2022.100639
- Lee S.J., Kim S., Simultaneous measurement of size and velocity of microbubbles moving in an opaque tube using an X-ray particle tracking velocimetry technique, *Experiments in Fluids*, 39 (2005) 492–497. DOI: 10.1007/s00348-005-0956-x
- Leighton T.G., *The Acoustic Bubble*, Academic Press, London, 1994, ISBN: 0-12-441921-6.
- Li M., Ma X., Eisener J., Pfeiffer P., Ohl C.-D., Sun C., How bulk nanobubbles are stable over a wide range of temperatures, *Journal of Colloid and Interface Science*, 596 (2021) 184–198. DOI: 10.1016/j.jcis.2021.03.064
- Liu G., Wu Z., J. Craig V.S.C., Cleaning of protein-coated surfaces using nanobubbles: an investigation using a quartz crystal microbalance, *The Journal of Physical Chemistry C*, 112 (2008) 16748–16753. DOI: 10.1021/jp805143c
- Liu G., J. Craig V.S.C., Improved cleaning of hydrophilic protein-coated surfaces using the combination of nanobubbles and SDS, *Applied Materials and Interfaces*, 1 (2009) 481–487. DOI: 10.1021/am800150p
- Liu S., Kawagoe Y., Makino, Y., Oshita, S., Effects of nanobubbles on the physicochemical properties of water: the basis for peculiar properties of water containing nanobubbles, *Chemical Engineering Science*, 93 (2013) 250–256. DOI: 10.1016/j.ces.2013.02.004
- Liu S., Oshita S., Makino Y., Wang Q., Kawagoe Y., Uchida T., Oxidative capacity of nanobubbles and its effect on seed germination, *ACS Sustainable Chemistry & Engineering*, 4 (2016a) 1347–1353. DOI: 10.1021/acssuschemeng.5b01368
- Liu S., Oshita S., Kawabata S., Makino Y., Yoshimoto T., Identification of ROS produced by nanobubbles and their positive and negative effects on vegetable seed germination, *Langmuir*, 32 (2016b) 11295–11302. DOI: 10.1021/acs.langmuir.6b01621
- Lohse D., Zhang X., Surface nanobubbles and nanodroplets, *Reviews of Modern Physics*, 87 (2015) 981–1035. DOI: 10.1103/RevModPhys.87.981
- Ma X., Li M., Pfeiffer P., Eisener J., Ohl C.-D., Ion adsorption stabilizes bulk nanobubbles, *Journal of Colloid and Interface Science*, 606 (2022) 1380–1394. DOI: 10.1016/j.jcis.2021.08.101

- Mai N.L., Koo Y.-M., Ha S.H., Separation characteristics of hydrophilic ionic liquids from ionic liquids-water solution by ultrasonic atomization, *Ultrasonics Sonochemistry*, 53 (2019) 187–191. DOI: 10.1016/j.ulsonch.2019.01.004
- Mason T.J., Ultrasonic cleaning: an historical perspective, *Ultrasonics Sonochemistry*, 29 (2016) 519–523. DOI: 10.1016/j.ulsonch.2015.05.004
- Matsuura K., Fukazu T., Abe F., Sekimoto T., Tomishige T., Efficient separation coupled with ultrasonic atomization using a molecular sieve, *AIChE Journal*, 53 (2007) 737–740. DOI: 10.1002/aic.11113
- Meegoda J.N., Hewage S.A., Batagoda J.H., Stability of nanobubbles, *Environmental Engineering Science*, 35 (2018) 1216–1227. DOI: 10.1089/ees.2018.0203
- Meegoda J.N., Hewage S.A., Batagoda J.H., Application of the diffused double layer theory to nanobubbles, *Langmuir*, 35 (2019) 12100–12112. DOI: 10.1021/acs.langmuir.9b01443
- Millare C.J., Basilia B.A., Nanobubbles from ethanol-water mixtures: generation and solute effects via solvent replacement method, *Chemistry Select*, 3 (2018) 9268–9275. DOI: 10.1002/slct.201801504
- Minamikawa K., Takahashi M., Makino T., Tago K., Hayatsu M., Irrigation with oxygen-nanobubble water can reduce methane emission and arsenic dissolution in a flooded rice paddy, *Environmental Research Letters*, 10 (2015) 084012. DOI: 10.1088/1748-9326/10/8/084012
- Morimatsu T., Goto M., Kohno M., Yabe A., Cleaning effect of nanobubbles (1st report: minute particle contamination), *Thermal Science and Engineering*, 12 (2004) 67–68.
- Muthukumar S., Kentish S., Lalchandani S., Ashokkumar M., Mawson R., Stevens G.W., Grieser F., The optimisation of ultrasonic cleaning procedures for dairy fouled ultrafiltration membranes, *Ultrasonics Sonochemistry*, 12 (2005) 29–35. DOI: 10.1016/j.ulsonch.2004.05.007
- Nakagawa M., Kioka A., Tagomori K., Nanobubbles as friction modifier, *Tribology International*, 165 (2022) 107333. DOI: 10.1016/j.triboint.2021.107333
- Nii S., Oka N., Size-selective separation of submicron particles in suspensions with ultrasonic atomization, *Ultrasonics Sonochemistry*, 21 (2014) 2032–2036. DOI: 10.1016/j.ulsonch.2014.03.033
- Nirmalkar N., Pacek A.W., Barigou M., On the existence and stability of bulk nanobubbles, *Langmuir*, 34 (2018a) 10964–10973. DOI: 10.1021/acs.langmuir.8b01163
- Nirmalkar N., Pacek A.W., Barigou M., Interpreting the interfacial and colloidal stability of bulk nanobubbles, *Soft Mater*, 14 (2018b) 9643–9656. DOI: 10.1039/c8sm01949e
- Nirmalkar N., Pacek A.W., Barigou M., Bulk nanobubbles from acoustically cavitating aqueous organic solvent mixtures, *Langmuir*, 35 (2019) 2188–2195. DOI: 10.1021/acs.langmuir.8b03113
- Ohgaki K., Khanh N.Q., Joden Y., Tsuji A., Nakagawa T., Physicochemical approach to nanobubble solutions, *Chemical Engineering Science*, 65 (2010) 1296–1300. DOI: 10.1016/j.ces.2009.10.003
- Patois E., Capelle M.A.H., Palais C., Gurny R., Arvinte T., Evaluation of nanoparticle tracking analysis (NTA) in the characterization of therapeutic antibodies and seasonal influenza vaccines: pros and cons, *Journal of Drug Delivery Science and Technology*, 22 (2012) 427–433. DOI: 10.1016/S1773-2247(12)50069-9
- Pétrier C., Lamy M.-F., Francony A., Benahcene A., David B., Sonochemical degradation of phenol in dilute aqueous solutions: comparison of the reaction rates at 20 and 487 kHz, *Journal of Physical Chemistry*, 98 (1994) 10514–10520. DOI: 10.1021/j100092a021
- Petsev N.D., Shell M.S., Leal L.G., Dynamic equilibrium explanation for nanobubbles' unusual temperature and saturation dependence, *Physical Review E*, 88 (2013) 010402. DOI: 10.1103/PhysRevE.88.010402
- Phan K., Truong T., Wang Y., Bhandari B., Effect of CO₂ nanobubbles incorporation on the viscosity reduction of fruit juice concentrate and vegetable oil, *International Journal of Food Science and Technology*, 56 (2021a) 4278–4286. DOI: 10.1111/ijfs.15240
- Phan K., Truong T., Wang Y., Bhandari B., Effect of electrolytes and surfactants on generation and longevity of carbon dioxide nanobubbles, *Food Chemistry*, 363 (2021b) 130299. DOI: 10.1016/j.foodchem.2021.130299
- Sakai T., Enomoto H., Torigoe K., Sakai H., Abe M., Surfactant- and reducer-free synthesis of gold nanoparticles in aqueous solutions, *Colloids and Surfaces A: Physicochemical and Engineering Aspects*, 347 (2009) 18–26. DOI: 10.1016/j.colsurfa.2008.10.037
- Sato M., Matsuura K., Fujii T., Ethanol separation from ethanol-water solution by ultrasonic atomization and its proposed mechanism based on parametric decay instability of capillary wave, *The Journal of Chemical Physics*, 114 (2001) 2382–2386. DOI: 10.1063/1.1336842
- Soyluoglu M., Kim D., Zaker Y., Karanfil T., Stability of oxygen nanobubbles under freshwater conditions, *Water Research*, 206 (2021) 117749. DOI: 10.1016/j.watres.2021.117749
- Stokes G.G., On the effect of the internal friction of fluids on the motion of pendulums, *Transactions of the Cambridge Philosophical Society*, 9 (1851) 8–106.
- Sugano K., Miyoshi Y., Inazato S., Study of ultrafine bubble stabilization by organic material adhesion, *Japanese Journal of Multiphase Flow*, 31 (2017) 299–306. DOI: 10.3811/jjmf.31.299
- Suslick K.S., *Sonochemistry*, Science, 247 (1990) 1439–1445. DOI: 10.1126/science.247.4949.1439
- Suzuki A., Maruyama H., Seki H., Matsukawa Y., Inoue N., Enrichment of amino acids by ultrasonic atomization, *Industrial & Engineering Chemistry Research*, 45 (2006) 830–833. DOI: 10.1021/ie0506771
- Tagomori K., Kioka A., Nakagawa M., Ueda A., Sato K., Yonezu K., Anzai S., Air nanobubbles retard calcite crystal growth, *Colloids and Surfaces A: Physicochemical and Engineering Aspects*, 648 (2022) 129319. DOI: 10.1016/j.colsurfa.2022.129319
- Takahashi M., ζ potential of microbubbles in aqueous solutions: electrical properties of the gas-water interface, *Journal Physical Chemistry B*, 109 (2005) 21858–21864. DOI: 10.1021/jp0445270
- Takahashi M., Shirai Y., Sugawa S., Free-radical generation from bulk nanobubbles in aqueous electrolyte solutions: ESR spin-trap observation of microbubble-treated water, *Langmuir*, 37 (2021) 5005–5011. DOI: 10.1021/acs.langmuir.1c00469
- Tanaka S., Naruse Y., Terasaka K., Fujioka S., Concentration and dilution of ultrafine bubbles in water, *Colloids and Interfaces*, 4 (2020) 50. DOI: 10.3390/colloids4040050
- Tanaka S., Kobayashi H., Ohuchi S., Terasaka K., Fujioka S., Destabilization of ultrafine bubbles in water using indirect ultrasonic irradiation, *Ultrasonics Sonochemistry*, 71 (2021a) 105366. DOI: 10.1016/j.ulsonch.2020.105366
- Tanaka S., Terasaka K., Fujioka S., Generation and long-term stability of ultrafine bubbles in water, *Chemie Ingenieur Technik*, 93 (2021b) 168–179. DOI: 10.1002/cite.202000143
- Terasaka K., Chapter 7—Cleaning with ultrafine bubble water, in: Terasaka K., Yasui K., Kanematsu W., Aya N. (Eds.), *Ultrafine Bubbles* (1st ed.), Jenny Stanford Publishing, 2021, pp. 179–190, ISBN: 9781003141952. DOI: 10.1201/9781003141952
- Tsuchida K., Maruyama A., Kobayashi Y., Sato G., Atsumi R., Murakami Y., Influence of microbubbles on free radical generation by ultrasound in aqueous solution: implication of the important roles of nanobubbles, *Research on Chemical Intermediates*, 48 (2022) 1045–1061. DOI: 10.1007/s11164-021-04612-6
- Tuziuti T., Yasui K., Kanematsu W., Variations in the size distribution of bulk nanobubbles in response to static pressure increases, *Japanese Journal of Applied Physics*, 59 (2020) SKKD03. DOI: 10.35848/1347-4065/ab78e5
- Tuziuti T., Yasui K., Kanematsu W., Influence of bulk nanobubble concentration on the intensity of sonoluminescence, *Ultrasonics Sonochemistry*, 76 (2021) 105646. DOI: 10.1016/j.ulsonch.2021.105646
- Ushida A., Hasegawa T., Nakajima T., Uchiyama H., Narumi T., Drag reduction effect of nanobubble mixture flows through micro-orifices and capillaries, *Experimental Thermal and Fluid Science*, 39 (2012a) 54–59. DOI: 10.1016/j.expthermfluidsci.2012.01.008
- Ushida A., Hasegawa T., Takahashi N., Nakajima T., Murao S., Narumi T., Uchiyama H., Effect of mixed nanobubble and microbubble liquids on the washing rate of cloth in an alternating flow, *Journal*

- of Surfactants and Detergents, 15 (2012b) 695–702. DOI: 10.1007/s11743-012-1348-x
- Ushikubo F.Y., Furukawa T., Nakagawa R., Enari M., Makino Y., Kawagoe Y., Shiina T., Oshita S., Evidence of the existence and the stability of nano-bubbles in water, *Colloids Surface A: Physicochemical and Engineering Aspects*, 361 (2010) 31–37. DOI: 10.1016/j.colsurfa.2010.03.005
- Wang Y., Pan Z., Luo X., Qin W., Jiao F., Effect of nanobubbles on adsorption of sodium oleate on calcite surface, *Minerals Engineering*, 133 (2019) 127–137. DOI: 10.1016/j.mineng.2019.01.015
- Wejjs J.H., Seddon J.R.T., Lohse D., Diffusive shielding stabilizes bulk nanobubble clusters, *Chem Phys Chem*, 13 (2012) 2197–2204. DOI: 10.1002/cphc.201100807
- Wood R.W., Loomis A.L., XXXVIII. The physical and biological effects of high-frequency sound-waves of great intensity, *The London, Edinburgh, and Dublin Philosophical Magazine and Journal of Science*, 4 (1927) 417–436. DOI: 10.1080/14786440908564348
- Wu Z., Chen H., Dong Y., Mao H., Sun J., Chen S., Craig V.S.J., Hu J., Cleaning using nanobubbles: defouling by electrochemical generation of bubbles, *Journal of Colloid and Interface Science*, 328 (2008) 10–14. DOI: 10.1016/j.jcis.2008.08.064
- Yabe A., Chapter 1—History of ultrafine bubbles, in: Terasaka K., Yasui K., Kanematsu W., Aya N. (Eds.), *Ultrafine Bubbles*, Jenny Stanford Publishing, 2021, pp. 1–16, ISBN: 9781003141952. DOI: 10.1201/9781003141952
- Yasuda K., Tanaka N., Rong L., Nakamura M., Li L., Oda A., Kawase Y., Effects of carrier gas conditions on concentration of alcohol aqueous solution by ultrasonic atomization, *Japanese Journal of Applied Physics*, 42 (2003) 2956–2957. DOI: 10.1143/JJAP.42.2956
- Yasuda K., Bando Y., Yamaguchi S., Nakamura M., Fujimori E., Oda A., Kawase Y., The effects of the solute properties in aqueous solutions on the separation characteristics in ultrasonic atomization, *Journal of Chemical Engineering of Japan*, 37 (2004) 1290–1292. DOI: 10.1252/jcej.37.1290
- Yasuda K., Honma H., Xu Z., Asakura Y., Koda S., Ultrasonic atomization amount for different frequencies, *Japanese Journal of Applied Physics*, 50 (2011) 07HE23. DOI: 10.1143/JJAP.50.07HE23
- Yasuda K., Nakayama S., Asakura Y., Characteristics of nanoemulsion prepared by tandem acoustic emulsification at a high frequency, *Journal of Chemical Engineering of Japan*, 45 (2012) 734–736. DOI: 10.1252/jcej.12we057
- Yasuda K., Mochida K., Asakura Y., Koda S., Separation characteristics of alcohol from aqueous solution by ultrasonic atomization, *Ultrasonics Sonochemistry*, 21 (2014) 2026–2031. DOI: 10.1016/j.ultrsonch.2014.02.011
- Yasuda K., Matsushima H., Asakura Y., Generation and reduction of bulk nanobubbles by ultrasonic irradiation, *Chemical Engineering Science*, 195 (2019) 455–461. DOI: 10.1016/j.ces.2018.09.044
- Yasuda K., Sato T., Asakura Y., Size-controlled synthesis of gold nanoparticles by ultrafine bubbles and pulsed ultrasound, *Chemical Engineering Science*, 217 (2020a) 115527. DOI: 10.1016/j.ces.2020.115527
- Yasuda K., Nohara Y., Asakura Y., Effect of ultrafine bubbles on ethanol enrichment using ultrasonic atomization, *Japanese Journal of Applied Physics*, 59 (2020b) SKKD09. DOI: 10.35848/1347-4065/ab83d9
- Yasuda K., Sonochemical green technology using active bubbles: degradation of organic substances in water, *Current Opinion in Green and Sustainable Chemistry*, 27 (2021) 100411. DOI: 10.1016/j.cogsc.2020.100411
- Yasuda K., Hamada K., Asakura Y., Enrichment of amino acids from its aqueous solution by ultrasonic atomization and ultrafine bubbles, *Japanese Journal of Applied Physics*, 61 (2022) SG1009. DOI: 10.35848/1347-4065/ac43e5
- Yasui K., Chapter 3—Dynamics of acoustic bubbles, in: Grieser F., Choi P.-K., Enomoto N. et al. (Eds.), *Sonochemistry and the Acoustic Bubble*, Elsevier, Amsterdam, 2015, pp. 41–83, ISBN: 9780128015308. DOI: 10.1016/B978-0-12-801530-8.00003-7
- Yasui K., Tuziuti T., Kanematsu W., Kato K., Advanced dynamic-equilibrium model for a nanobubble and a micropancake on a hydrophobic or hydrophilic surface, *Physical Review E*, 91 (2015) 033008. DOI: 10.1103/PhysRevE.91.033008
- Yasui K., Tuziuti T., Kanematsu W., Kato K., Dynamic equilibrium model for a bulk nanobubble and a microbubble partly covered with hydrophobic material, *Langmuir*, 32 (2016) 11101–11110. DOI: 10.1021/acs.langmuir.5b04703
- Yasui K., *Acoustic Cavitation and Bubble Dynamics*, Springer, Cham, Switzerland, 2018, ISBN: 9783319682372. DOI: 10.1007/978-3-319-68237-2
- Yasui K., Tuziuti T., Kanematsu W., Mysteries of bulk nanobubbles (ultrafine bubbles); stability and radical formation, *Ultrasonics Sonochemistry*, 48 (2018) 259–266. DOI: 10.1016/j.ultrsonch.2018.05.038
- Zhang R., Gao Y., Chen L., Ge G., Nanobubble boundary layer thickness quantified by solvent relaxation NMR, *Journal of Colloid and Interface Science*, 609 (2022a) 637–644. DOI: 10.1016/j.jcis.2021.11.072
- Zhang R., Gao Y., Chen L., Ge G., Controllable preparation of monodisperse nanobubbles by membrane sieving, *Colloids and Surfaces A: Physicochemical and Engineering Aspects*, 642 (2022b) 128656. DOI: 10.1016/j.colsurfa.2022.128656
- Zhang X., Liu X., Zhong Y., Zhou Z., Huang Y., Sun C.Q., Nanobubble skin supersolidity, *Langmuir*, 32 (2016) 11321–11327. DOI: 10.1021/acs.langmuir.6b01660
- Zhou Y., Han Z., He C., Feng Q., Wang K., Wang Y., Luo N., Dodbiba G., Wei Y., Otsuki A., Fujita T., Long-term stability of different kinds of gas nanobubbles in deionized and salt water, *Materials*, 14 (2021) 1808. DOI: 10.3390/ma14071808
- Zhu J., An H., Alheshibri M., Liu L., Terpstra P.M.J., Liu G., Craig V.S.J., Cleaning with bulk nanobubbles, *Langmuir*, 32 (2016) 11203–11211. DOI: 10.1021/acs.langmuir.6b01004
- Zimmerman W.B., Tesar V., Bandulasena H.C.H., Towards energy efficient nanobubble generation with fluidic oscillation, *Current Opinion in Colloid & Interface Science*, 16 (2011) 350–356. DOI: 10.1016/j.cocis.2011.01.010

Author's Short Biography



Keiji Yasuda

Keiji Yasuda is currently an Associate Professor of the Department of Chemical Systems Engineering, Nagoya University. He received Doctor degree of Engineering from Nagoya University in 1997. His research interests are in the area of fundamentals of fine bubbles and sonochemistry, and their application to material and environmental fields.